Application Note – *In Situ* Pulse Voltammetry of PEM Fuel Cell Electrodes with Scribner Model 885-HS Potentiostat

Introduction

This application note briefly demonstrates the use of Scribner's Model 885-HS Fuel Cell Potentiostat for pulse voltammetry for polymer electrolyte membrane (PEM) fuel cells. The 885-HS Fuel Cell Potentiostat was specifically designed for use and integration with Scribner's 850/890 Fuel Cell Test Systems and *FuelCell*® software for hands-free switching between standard fuel cell operating mode and diagnostics methods that require a potentiostat, such as linear sweep voltammetry for fuel crossover and cyclic voltammetry for electrochemical surface area (ECSA) analysis. The 885-HS features 100 pt/s data acquisition rate, 2 A current rating, and seamless integration with *FuelCell*® software.

Zawodzinski and co-workers recently introduced pulse voltammetry of PEM fuel cell electrodes as a new approach to measuring *in situ* the oxide coverage on platinum and platinum alloy catalysts under simulated operating conditions (1-3) and electrode kinetics (4).

If successful, *in situ* pulse voltammetry of fuel cell electrodes has the advantage that electrode properties can be measured under actual or simulated fuel cell operating conditions. For example, the oxidation behavior of Pt and Pt-alloy catalyst *in a fuel cell electrode* can be characterized as a function of temperature and relative humidity (1, 2), which is not feasible in a traditional wet chemistry setup. In addition, because pulse voltammetry is very sensitive to the electrode surface condition, such as the presence of an electrochemically-active adsorbed species or an oxide, the technique may provide new insight into the potential window at which reactions occur. For example, enhanced understanding of the potential regime at which platinum oxides form, the conditions that favor or inhibit oxidation/reduction processes, and the effect of alloying additions, could inform selection of the optimal fuel cell operating conditions and catalyst composition.

The application of pulse voltammetry to PEM fuel cell electrodes is limited by the large non-faradaic double-layer charging current that results from the voltage-step of the large capacitance electrode. Most commercial potentiostats have a current limit of ~ 2 A, so pulse voltammetry is limited to relatively small PEM fuel cells, *e.g.*, 5 cm^2 or less.

Here, we demonstrate the use of Scribner's fuel cell test equipment, in particular the Model 885-HS Fuel Cell Potentiostat for *in situ* pulse voltammetry of PEM fuel cell electrodes.

Experimental

In this work, we used a 5 cm^2 Gore PRIMEA® Series 57 membrane electrode assembly (0.4 mg/cm^2 Pt on anode and cathode) and SGL SIGRACET® 25BC gas diffusion layers in Scribner single cell hardware. The fuel cell cathode was fed N_2 and was the working electrode while the fuel cell anode was fed H_2 and acted as the counter and pseudo-reference electrode.

The fuel cell's environmental conditions were controlled with a Scribner 850e Fuel Cell Test System and *FuelCell*® software. Cell temperature was 80 ^oC and the desired relative humidity (RH) was achieved by setting the anode and cathode humidifier temperature to 49.2 ^oC for 25% RH, 64 ^oC for 50% RH or 80 ^oC for 100% RH. All tests were performed at ambient pressure.

Pulse voltammograms were obtained with a Model 885-HS Fuel Cell Potentiostat (2 A max. current) controlled by *FuelCell*® software at 100 pts/s. The pulse voltammograms consisted of a series of constant-voltage experiments executed sequentially.

Detection of Catalyst Oxidation by Normal Pulse Voltammetry

Normal Pulse Voltammetry consists of applying a series of increasing voltage steps E_{pulse} to the working electrode with a return to a base potential E_{base} between each pulse in order to return the electrode surface to a consistent condition. The voltage waveform and resulting current profile is illustrated in Figure 1 where t_p is the pulse width and t_w is the wait time at E_{base} between pulses. The current at the end of the pulse period is recorded and plotted as a function of the pulse voltage.

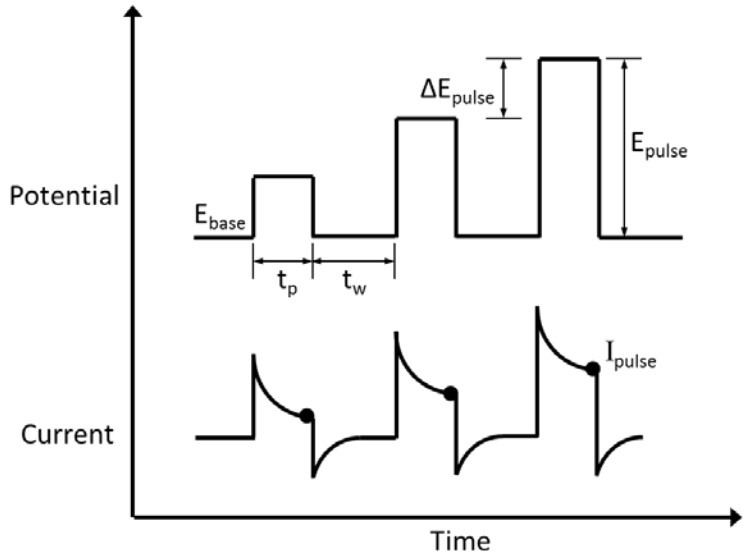

Figure 1. Illustration of the potential and current response during a normal pulse voltammetry experiment. The pulse current is measured at the end of the pulse period t_p.

Figure 2 shows a typical voltage and current profile for the normal pulse voltammetry experiment. At each voltage step, there was a large current transient predominately due to capacitive charging of the electrode double layer. In analyzing the voltammogram, the current at the end of the potential pulse, when the non-faradaic charging current was smallest, was plotted as a function of the pulse potential.

In situ pulse voltammograms of the 5 cm^2 PEM fuel cell are shown in Figure 3. Four plots are shown demonstrating the effect of the wait time t_w at E_{base} and the pulse duration t_p at E_{pulse}. For the pulse durations examined here, changing the length of the hold at the base potential from 1 to 5 s did not have any influence. This result indicates that any chemical reactions that occurred during the pulse step were fully reversed within the first second of the subsequent hold at the base potential.

The form of the voltammogram changed slightly when the pulse width was increased from 1 to 2 s. Overall, the pulse current was smaller for the longer pulse period, indicating that there was some residual double-layer capacitance charging current at 1 s, which has further decayed after 2 s.

An initial oxidation onset potential ~ 0.625 V is evident as a change in slope and has been attributed to the formation of platinum hydroxide (PtOH) (1, 2).

$$Pt + H_2O \rightarrow PtOH + H^+ + e^-$$

It is generally considered that this reaction occurs at potentials more positive than ~ 0.85 V (5). The results presented here are consistent with those of Zawodzinski *et. al.* (1, 2) and are a consequence of the higher sensitivity of the pulse voltammetry technique.

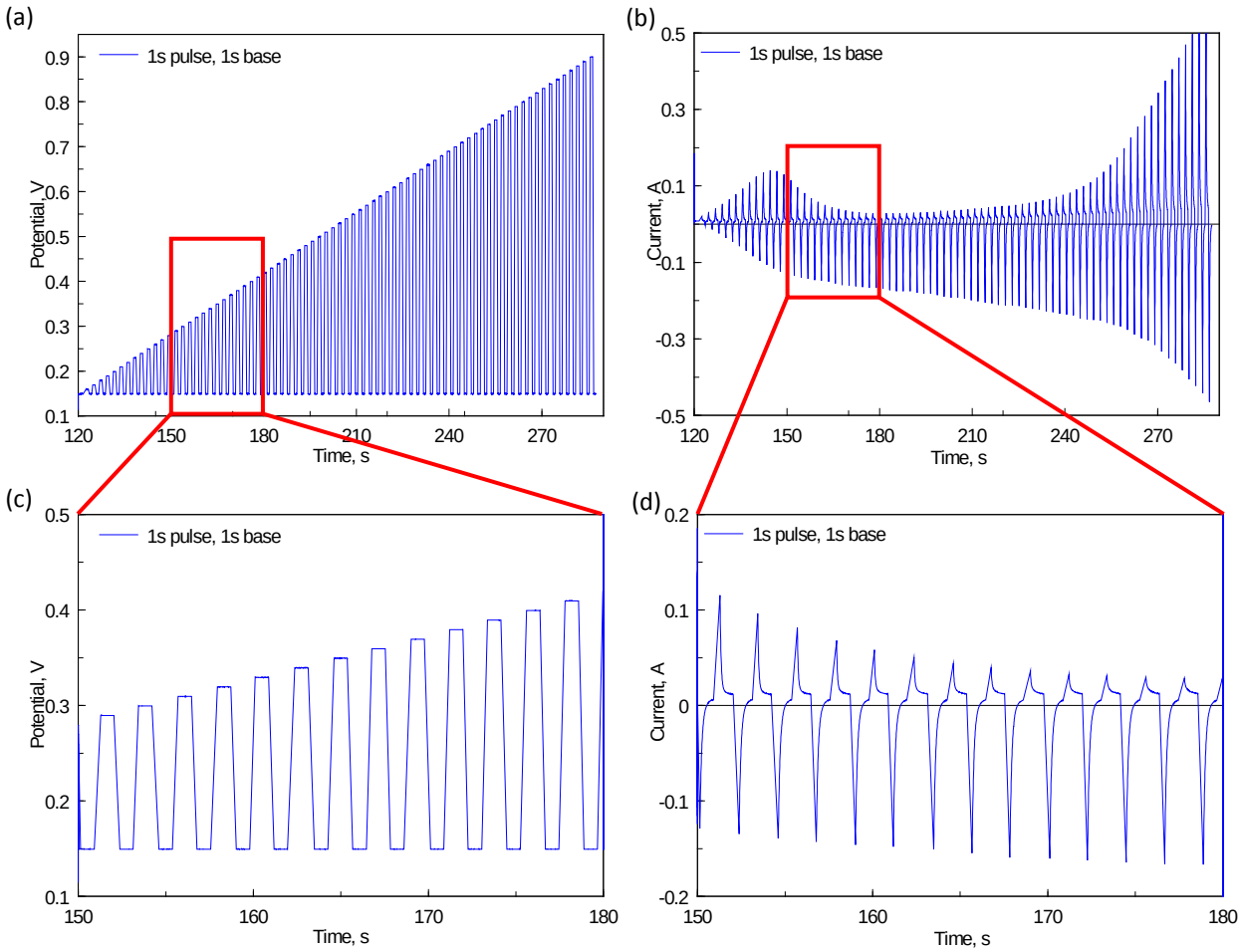

Figure 2. Voltage and current profiles during *in situ* normal pulse voltammetry of PEM fuel cell electrode. E_{base} = 0.15 V, ΔE_{pulse} = 0.01 V, E_{max} = 0.9 V, $t_p = t_w$ = 1 s. Cell conditions: 80 °C, 50% RH, 0.3 SLM H_2 / 0.5 SLM N_2.

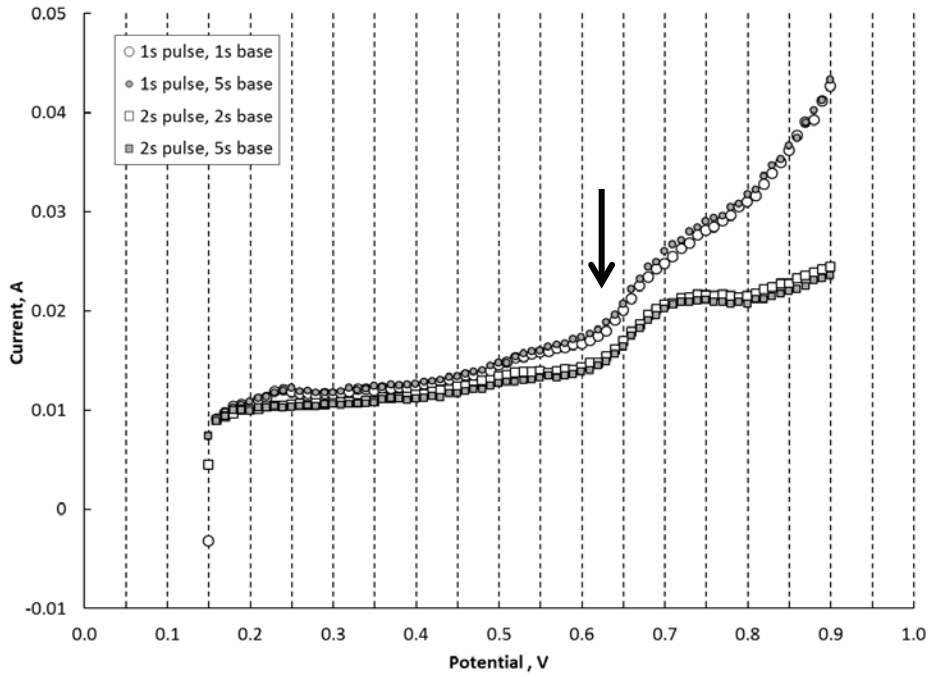

Figure 3. Normal pulse voltammograms of a Pt catalyst PEM fuel cell showing the influence of pulse width (t_p = 1 or 2 s) and base potential wait time (t_w = 1, 2 or 5 s). E_{base} = 0.15 V, ΔE_{pulse} = 10 mV, E_{max} = 0.9 V. Conditions: 0.1 SLM H_2 anode / 0.12 SLM N_2 cathode, 80 ^oC, 100% RH.

Oxide Stripping by Pulse Voltammetry

It is well established that platinum oxidizes at potentials that are commonly experienced by the air electrode in a PEM fuel cell. Platinum oxide (PtO) can form at potentials above 1.1 V *vs*. reversible hydrogen electrode (RHE) whereas platinum hydroxide (PtOH) is generally considered to form between 0.85 and 1.1 V. Platinum is thought to be oxide-free at potentials less than ~ 0.85 V (6).

For the *in situ* oxide stripping experiments by pulse voltammetry, the working electrode (fuel cell cathode) is held for various durations at a potential where oxidation of the platinum occurs before stepping the electrode potential to a low value in order to reduce the Pt-oxide. The oxide reduction current and charge are monitored and evaluated as a function of the time at the high oxidizing potential.

The waveform consisted to two components: (*i*) an initial oxide formation or conditioning step at 0.98 V which lasted 1 to 10,000 seconds followed by (*ii*) oxide stripping step at 0.6 V for 120 seconds. This is shown in Figure 4. Representative raw voltage and current time profiles for the voltage pulse experiment are shown in Figure 5.

During the period immediately after the voltage step (< ~ 1 s), there was a large current transient due to non-faradaic charging of the double layer. By design, PEM fuel cell electrodes have very large true surface area and consequently large double layer capacitance. For example, the PEM MEA with nominal 5 cm^2 area used in this work displayed double layer capacitance ~ 0.15 F. The double layer charging current is proportional to its capacitance C_{dl} and the rate of change of the voltage dV/dt across the electrode interface,

$$I_{dl} = C_{dl}\frac{dV}{dt}$$

Large double layer capacitance begets large double layer charging current.

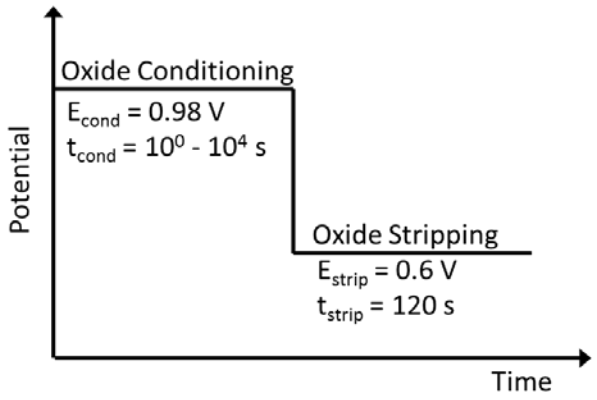

Figure 4. Illustration of the pulse voltammetry waveform for *in situ* characterization of oxide formation at a PEM fuel cell electrode with Pt catalyst. The oxide conditioning step at 0.98 V lasted 1 to 10,000 s and was followed by a 120 s oxide stripping step at 0.6 V.

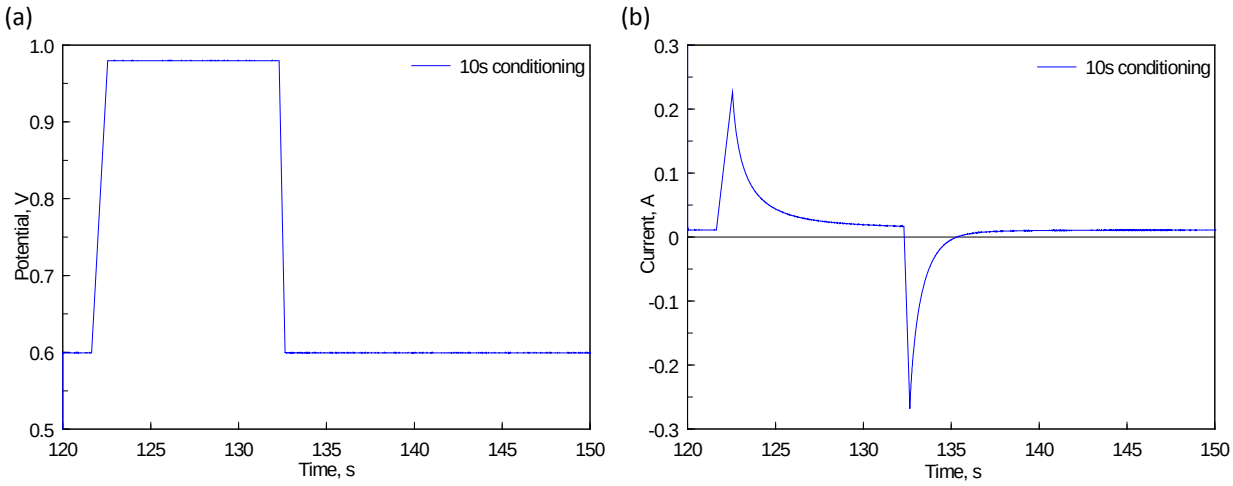

Figure 5. Voltage (a) and current (b) *vs.* time for oxide stripping experiments. E_{cond} = 0.98 V, t_{cond} = 10 s, E_{strip} = 0.6 V, t_{strip} = 120 s. The conditioning step was preceded by potentiostatic hold at 0.6 V. The constant positive current ~ 0.01 A at long times after the voltage step was due to oxidation of H_2 crossover. Cell conditions: 80 °C, 50% RH, 0.3 SLM H_2 anode / 0.5 SLM N_2 cathode.

In contrast, the steady-state positive current at long times is due to oxidation of H_2 at the working electrode. Superimposed on the capacitive charging current and H_2 crossover current is the current due to Pt oxidation during the conditioning step at E_{cond} = 0.98 V or the reduction of Pt-oxide during the subsequent stripping step at E_{strip} = 0.6 V. The goal is to correct the overall observed response for the combined effects of the capacitive charging and H_2 crossover in order to reveal the current and charge associated with the Pt-oxide reduction.

The current due to H_2 crossover was calculated as the average current over the last 30 s of the oxide stripping step at 0.6 V. The chronoamperometric and chronocoulombic responses shown in Figure 6 were corrected by subtracting the H_2 oxidation current at all points.

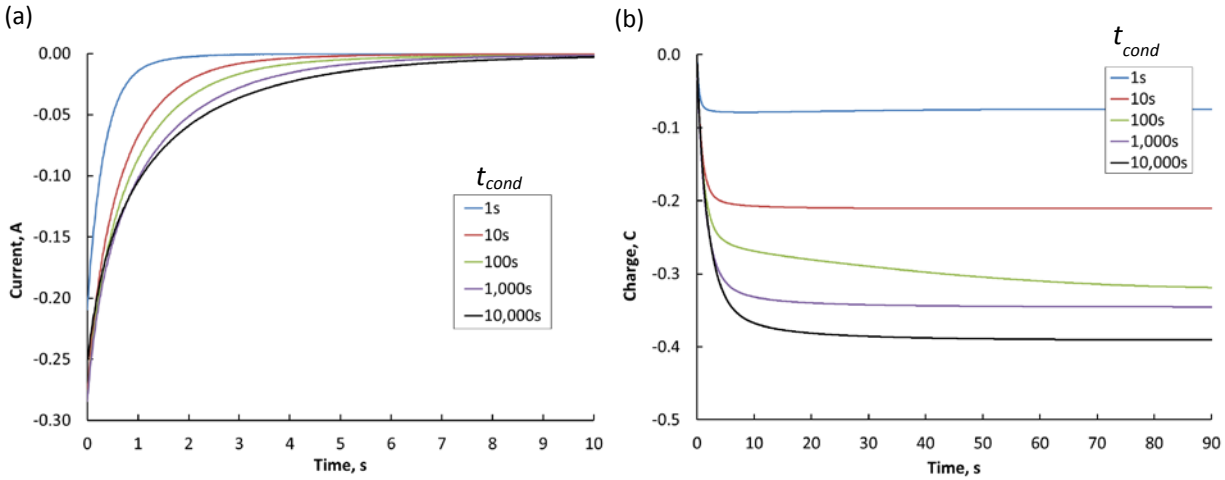

Figure 6. Current (a) and charge (b) *vs*. time for a potential step from 0.98 V to 0.6 V measured *in situ* for a PEM fuel cell electrode. High initial currents are non-faradaic capacitive charging of the electrode double layer. The oxide reduction current and charge increase as oxide growth time at 0.98 V increased from t_{cond} = 1 to 10,000 s. Current and charge were corrected for H_2 crossover. Cell conditions as in Figure 5.

The charge is re-plotted on a semi-log format in Figure 7(a) to highlight the time just after the voltage step, t_{strip} < 1 s. In this region, the current is dominated by capacitive effects. The effect of oxide conditioning time only becomes evident at strip times greater than ~ 2 s.

To account for capacitive effects, we assume that the shortest oxide conditioning time t_{cond} = 1 s has negligible surface oxidation and therefore is representative of the capacitive contribution to the total current. The current and charge obtained for the stripping of the 10 to 10,000 s conditioning steps were therefore corrected for capacitive contribution by subtracting the stripping current and charge for the 1 s conditioning step. This background-corrected data is summarized in Figure 7(b).

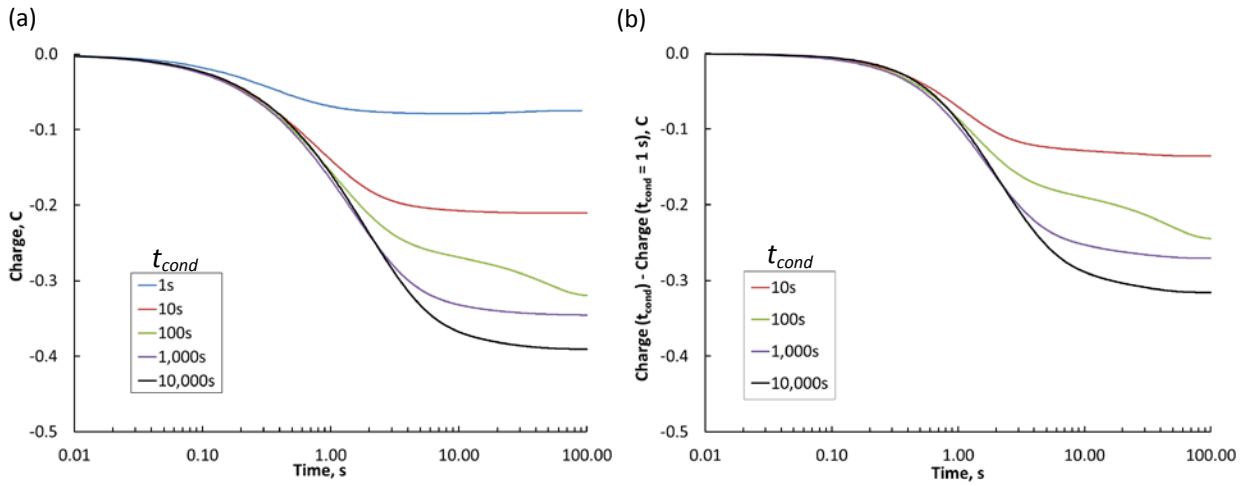

Figure 7. (a) Crossover-corrected charge *vs*. log time for a potential step from 0.98 V to 0.6 V measured *in situ* for a PEM fuel cell electrode. The log scale highlights the capacitive effect at very short times (< 1 s) and the oxide stripping charge at short to intermediate times (< 10 s). (b) Charge due to oxide reduction using the 1 s oxide formation condition (t_{cond} = 1 s) as the background charge to correct for capacitive effects. The oxide reduction charge increased as the conditioning time at 0.98 V increased from t_{cond} = 10 to 10,000 s. Cell conditions as in Figure 5.

Figure 8 shows the oxide stripping charge (corrected for capacitive charging and H_2 crossover effects) *vs*. the logarithm of the oxide formation time (log t_{cond}) for a Pt-catalyst based PEM fuel cell electrode at 25% and 50% RH. The slope reflects the oxide reduction charge per decade of conditioning time. Higher humidity resulted in greater oxide reduction charge: 32.5 *vs*. 27.4 mC/dec at 50% and 25% RH, respectively. The results are consistent with those presented in reference (4), who noted that the humidity dependence of the oxidation indicates that water is involved in Pt → PtOH reaction.

Conclusions

We have demonstrated an experimental method to measure in situ platinum oxide growth and coverage on PEM fuel cell electrodes under simulated operating conditions. Integration of the 885-HS Fuel Cell Potentiostat with the 850/890 Fuel Cell Test System and *FuelCell*® software facilitate easy, user-friendly implementation of the wide array of pulse voltammetry methods for in situ characterizing of PEM fuel cell electrodes under real and simulated operating conditions.

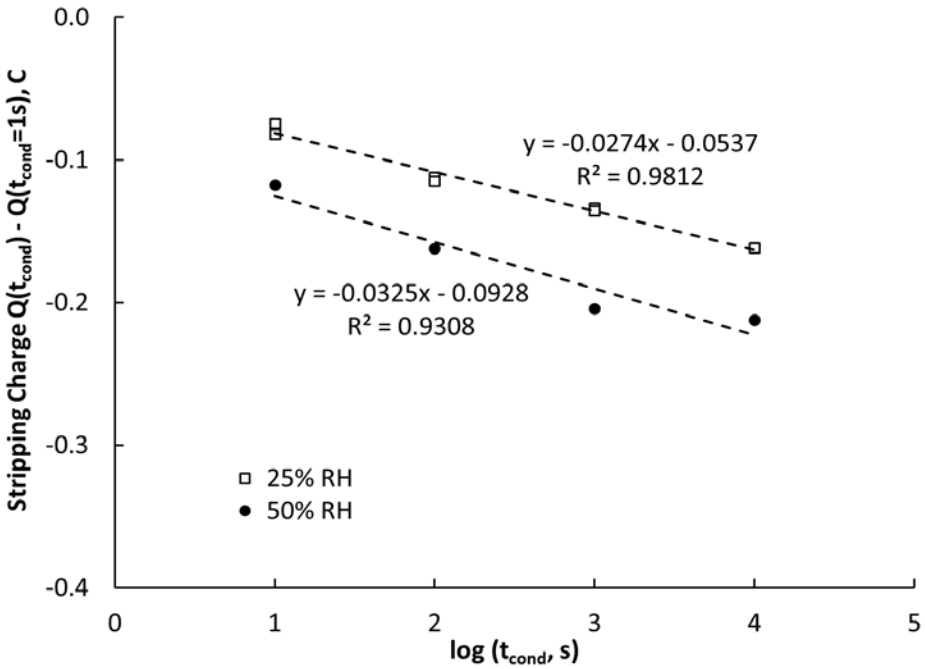

Figure 8. Oxide stripping charge at t_{strip} = 3.16 s (*i.e.*, log t_{strip} = 0.5) *vs.* log oxide formation time (log t_{cond}) for a Pt-catalyst based PEM fuel cell electrode at 25% (□) and 50% RH (●). The slope reflects the oxide reduction charge per log (time). Higher humidity was associated with higher oxide reduction charge, *i.e.*, 32.5 mC/log(s) at 50% RH *vs.* 27.4 mC/log(s) at 25% RH). Cell conditions as in Figure 5.

References

1. P. Pietrasz, R. M. Sankaran and T. A. Zawodzinski, "Pulse Voltammetry [of Alloy Metal Catalysts] at Fuel Cell Electrodes," *ECS Transactions*, 2008, **16**, 1583-1589.
2. P. Pietrasz and T. A. Zawodzinski, "Pulse Voltammetry Investigations of Platinum Metal Fuel Cell Electrodes," *ECS Transactions*, 2009, **25**, 635-641.
3. P. A. Stuckey, P. Pietrasz and T. A. Zawodzinski, "Normal Pulse Voltammetry: *in situ* Kinetic Analysis of Proton Exchange Membrane Fuel Cells," *ECS Transactions*, 2010, **33**, 1309-1319.
4. P. A. Stuckey and T. A. Zawodzinski, "Pulse Voltammetry: *in situ* Measurements of Oxide Coverage on Platinum in Proton Exchange Membrane Fuel Cells," *ECS Transactions*, 2011, **41**, 651-660.
5. A. K. N. Reddy, M. A. Genshaw and J. O. M. Bockris, *Journal of Chemical Physics*, 1968, **48**, 671.
6. M. Teliska, V. S. Murthi, S. Mukerjee and D. E. Ramaker, "Correlation of Water Activation, Surface Properties, and Oxygen Reduction Reactivity of Supported Pt–M/C Bimetallic Electrocatalysts Using XAS," *Journal of the Electrochemical Society*, 2005, **152**, A2159-A2169.

